International Journal of Mass Spectrometry 199 (2000) 17–27

Photoionization of methyl *t*-butyl ether (MTBE) and *t*-octyl methyl ether (TOME) and analysis of their pyrolyses by supersonic jet/photoionization mass spectrometry

Steven D. Chambreau[a], Jingsong Zhang[a,b], John C. Traeger[c], Thomas Hellman Morton[a,]*

[a]*Department of Chemistry, University of California, Riverside, CA 92521, USA*
[b]*Air Pollution Research Center, University of California, Riverside, CA 92521, USA*
[c]*Department of Chemistry, La Trobe University, Bundoora, Victoria 3083, Australia*

Received 13 May 1999; accepted 20 July 1999

Abstract

The pyrolysis products of neutral methyl-d_3 *t*-butyl ether (MTBE-d_3), its undeuterated analogue, and *t*-octyl methyl ether (TOME) have been analyzed by means of supersonic jet expansion followed by 118 nm photoionization/time-of-flight mass spectrometry. The mass spectra recorded for pyrolysis temperatures up to 1200 °C are compared with the photoionization efficiency (PIE) of room temperature samples as a function of photon energy in the domain 9–13 eV. Differences in fragment ion abundances measured by the two techniques permit the dissection of ion decomposition profiles away from thermal cracking patterns. MTBE and TOME both exhibit base peaks at *m/z* 73 (which shifts to *m/z* 76 for MTBE-d_3). For neutral MTBE at room temperature, supersonic expansion followed by 118 nm photoionization of the jet-cooled molecular beam gives a mass spectrum in which the molecular ion appears with approximately 10% the abundance of the base peak, a much higher relative intensity than is seen for the molecular ion at any wavelength when the neutral precursor is photoionized at room temperature. Pyrolysis of MTBE leads to molecular elimination of methanol as the only observed thermal decomposition (in agreement with previous studies) up to roughly 1000 °C. At temperatures $\geq$1050 °C, however, detectable levels of bond homolysis take place, as revealed by the production of both $CH_3\cdot$ and $CD_3\cdot$ (observed as *m/z* 15 and 18 in the photoionization mass spectra) from $(CH_3)_3COCD_3$. This result is consistent with the expectation that bond homolysis should have an Arrhenius preexponential factor $>$100 times greater than that for molecular elimination, which compensates for the 0.9 eV higher energy barrier difference at sufficiently elevated temperatures. TOME also displays molecular elimination, but the prevalence of homolysis in the resulting alkenes (2,4,4-trimethylpentenes) prevents assessment of direct bond homolysis in TOME. (Int J Mass Spectrom 199 (2000) 17–27) © 2000 Elsevier Science B.V.

Keywords: Acetone; Antiknock; Fuel additive; Homolysis; Methyl radical; Oxygenate

---

* Corresponding author. E-mail: morton@citrus.vcr.edu

Dedicated to Henri Audier on the occasion of his 60th birthday.

PII S1387-3806(00)00168-8

1. Introduction

t-Alkyl methyl ethers possess excellent antiknock characteristics in motor fuel [1]. Nevertheless, the most commonly used gasoline additives—methyl *t*-butyl ether (MTBE) and *t*-amyl methyl ether (TAME)—have the undesirable property of being moderately water-soluble. As a consequence, leakages from underground storage tanks and fuel pipelines pose a serious hazard to ground water, threatening to pollute drinking supplies with organic compounds that cannot be readily degraded biologically.

One potential solution is to use higher homologues, such as *t*-octyl methyl ether (TOME, 2-methoxy-2,4,4-trimethylpentane), which is much less water-soluble. On a mole-per-mole basis TOME displays better antiknock properties than MTBE [1]. Moreover, it can be synthesized at the oil refinery from the same feedstocks as used to make MTBE: isobutene and methanol. The manufacture of MTBE employs acid catalysts to promote Markownikoff addition of methanol to the double bond. By changing stoichiometry (2 moles of isobutene per mole of methanol) the same general route could be used to prepare TOME.

In an engine, fuel additives experience high temperatures for short contact times. Under such conditions, mechanisms with very different activation energies may compete with one another, provided that the pathway with the higher barrier has a more favorable Arrhenius preexponential factor. *t*-Alkyl methyl ethers represent a case in point. Simple bond fissions to form free radicals typically have much higher activation barriers than molecular elimination. Yet, to judge by more than a half-dozen published reports on the pyrolysis of neopentane [2,3], the preexponential factor for C–C bond homolysis is $A > 10^{16}\ \mathrm{s}^{-1}$. While this high value for the A factor has not gone unchallenged [4], it is more than 100 times greater than the A factor for molecular elimination in neutral MTBE (Eq. (1) [5]). If methyl cleavage in neutral MTBE also exhibits a large A value, then it ought to be observed in competition with molecular elimination at temperatures above 1000 °C. Direct generation of radicals may, in turn, influence the combustion chemistry of fuel additives. We present evidence for C–C bond homolysis in MTBE.

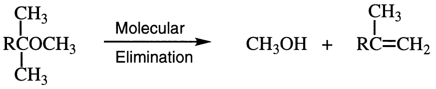

$$\mathrm{R\overset{CH_3}{\underset{CH_3}{C}}OCH_3} \xrightarrow[\text{Elimination}]{\text{Molecular}} \mathrm{CH_3OH} + \mathrm{R\overset{CH_3}{C}{=}CH_2} \qquad (1)$$

MTBE: $\mathrm{R{=}CH_3}$
TOME: $\mathrm{R{=}(CH_3)_3CCH_2}$

The present work makes use of mass spectrometry to analyze the products from heating (400–1200 °C) MTBE and TOME on the microsecond timescale. Little has been published regarding the pyrolytic degradation or mass spectrometry of TOME. One might imagine that neutral TOME should exhibit the same unimolecular reactions as does neutral MTBE, which (under homogeneous conditions in the gas phase) undergoes molecular elimination to yield methanol and isobutene [5] (the molecules from which MTBE is usually assembled). Here we report the parallelism between MTBE and TOME, although homolysis of TOME's decomposition products prevents observation of direct C–C fission of that ether.

2. Experimental

Thermal decomposition experiments were performed in the apparatus schematically depicted in Fig. 1, which uses a Wiley–MacLaren type linear time-of-flight (TOF) mass spectrometer (TOFMS, model D-651, R. M. Jordan Company) to monitor pyrolysis products by 118 nm photoionization. The main reaction chamber was pumped by a cryobaffled Varian VHS-6 diffusion pump, and the mass spectrometer (MS) was differentially pumped with a turbomolecular pump and a liquid nitrogen trap. Pyrolyses were carried out by expanding the parent molecules, seeded in helium or argon, through a heated silicon carbide tube (Carborundum Corp.) into the photoionization region of the MS, similar to the apparatus described by Chen and co-workers [6]. A 1 mm i.d. silicon carbide tube was attached to a machinable piece of alumina (which was mounted to the faceplate of a General Valve series 9 pulsed valve) by means of a high temperature ceramic adhesive (Cotronics Corporation). The alumina piece insulated the silicon car-

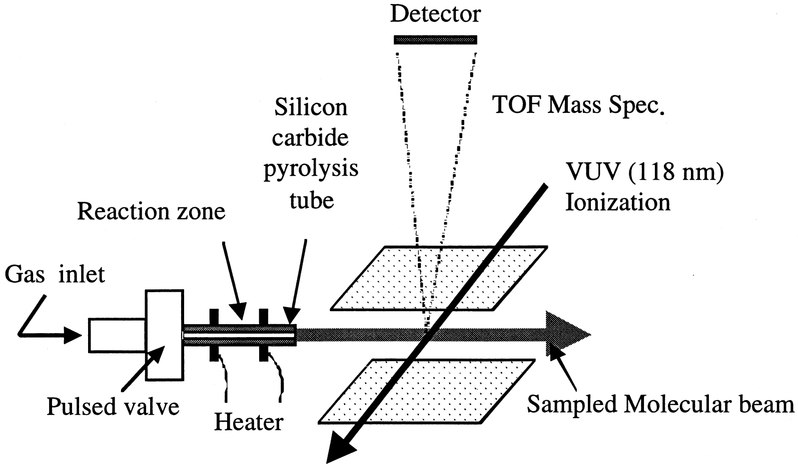

Fig. 1. Schematic of the pyrolysis/supersonic jet expansion/photoionization/time-of-flight mass spectrometer apparatus used to observe thermal decomposition products.

bide tube (2 mm o.d.) both thermally and electrically from the pulsed valve and was attached to an aluminum plate to provide additional mechanical stability. Two graphite electrodes (Poco Graphite), separated by 1 cm, were press fitted onto the silicon carbide tube, and current was run through the tube to heat it resistively. Electrical current was controlled with a Variac transformer, and nominal temperature was monitored with a type C thermocouple (Omega) wrapped around the outside of the heated portion of the silicon carbide nozzle. A temperature calibration curve was plotted by inserting a thermocouple insulated with ceramic adhesive into the heated nozzle and comparing that reading (T_{internal}) with the nominal temperature (T_{nominal}), which gives the empirical relation

$T_{\text{internal}} = 1.23 \quad T_{\text{nominal}} - 60\ °\text{C}$ for $T_{\text{nominal}} \geq$ 400 °C. Heat dissipation by the inserted thermocouple may have a greater cooling effect than the gas pulse, so the calibration equation represents only a best approximation, and nominal temperatures are reported in Figs. 3 and 5. The residence time of the parent molecules within the heated region was estimated to be on the order of 10^{-5} s.

After exiting from the heated zone the unreacted precursor and its products were cooled by supersonic expansion. The degree of cooling increases with the mass of the monoatomic carrier gas, and the rotational temperature of molecules in the jet after expansion is ≤ -230 °C, as has been ascertained by Chen and co-workers [7] by means of multiphoton ionization (although the vibrational temperature tends to be somewhat higher). The present studies were performed using both helium and argon as carrier gases, but only the latter results are described below.

Pyrolysis products were ionized by single photon ionization at 118 nm (10.45 eV) using the frequency tripled third harmonic (355 nm) of a Nd-YAG laser output in a low pressure (6.5×10^3 Pa) Xe cell attached directly to the vacuum chamber. The 118 nm light was focused into the chamber with a MgF_2 lens, and the intensity at this wavelength was maximized by measuring the photoionization of NO (IE = 9.2 eV) in an ionization cell located at the back of the chamber. The ion current produced was measured as a voltage drop between two electrode plates within the cell biased at 0 and +180 V. Alignment of the molecular beam and the photoionizing radiation were optimized by changing the positions of the 355 nm focusing lenses and the molecular beam nozzle and by varying the delay time between the molecular beam pulse and the laser firing so to give a maximum intensity mass peak when running pure NO (*m/z* 30) through the molecular beam nozzle. Data were averaged on a HP54502A digital oscilloscope (400 MHz) and recorded with LabView software. The sampling rate was 10 Hz, and the molecular beam pulse width was 0.2 ms. Individual spectra were recorded averages of 160 laser shots, and groups of individual spectra were summed to improve signal-to-noise. A small amount of ionization takes place as a result of electrons that are generated from metal surfaces by the photoelectric effect and accelerated by the electric field. These produce *m/z* 40 ions from the argon carrier gas at intensities approximately one-fourth that of the base peak from the organic substrate, as well as a much smaller *m/z* 20 peak corresponding to Ar^{++}. Peaks from argon are subtracted from the spectra reproduced in Figs. 3 and 5.

MTBE and trimethylpentene samples were purchased from Aldrich, and MTBE-d_3 was purchased from Cambridge Isotope Laboratories. These were used without further purification. TOME was synthesized by $H_2SO_4/MgSO_4$-catalyzed addition of methanol to 2,4,4-trimethyl-1-pentene (by analogy to the published method for preparing *t*-butyl ethers [8]) and purified by repeated distillations. Nevertheless a few percent of residual starting material (in an equilibrium mixture with its less stable isomer 2,4,4-trimethyl-2-pentene in an approximately 85:15 ratio [9]) remained in the TOME sample and was used for estimating the thermal decomposition of TOME's molecular elimination products. All samples were introduced into the pyrolysis apparatus with the carrier gas (helium or argon) pressure at 1.3×10^5 Pa, which was bubbled through the samples maintained at 0 °C prior to introduction into the chamber.

Photoionization efficiency (PIE) curves were measured on an apparatus that has been described elsewhere [10–12]. The source of a microcomputer-controlled magnetic sector mass spectrometer makes use of the hydrogen pseudocontinuum and a Seya–Namioka monochromator equipped with a holographically ruled diffraction grating. Resolution of the monochromator was fixed at 1.35 Å, and the absolute energy scale was calibrated with atomic emission lines to an accuracy of better than 0.003 eV. All experiments were performed at ambient temperature (24 °C) with sample pressures of 10^{-3} Pa in the ion-source region. Experimental PIE curves were analytically smoothed with a Fourier transform filter using the program HORIZON (Star Blue Software, Inc.). The 298 K appearance energies (AEs) were obtained from a simple linear extrapolation of the PIE curves in the threshold region. Density functional theory (DFT) calculations on molecular fragments were performed using GAUSSIAN98 on the Cray T90 at the San Diego Supercomputing Center.

3. Results

The methodology for the thermal decomposition studies involved cooling the pyrolysis products in a supersonic jet of inert gas, followed by photoionization/TOF mass spectrometry. Therefore we also describe the photoionization mass spectra of room temperature samples MTBE and TOME as a function of wavelength, in order to dissect the consequences of simply heating the neutral versus decomposing it. As has been well documented, MTBE does not give an intense molecular ion peak, but loses methyl, as summarized in Eq. (2) for MTBE-d_3 [13]. Ionized TOME exhibits the same type of decompositions, but methyl loss competes with loss of a neopentyl radical.

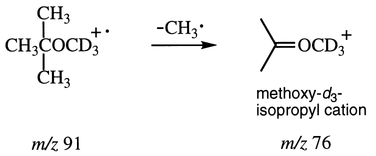

(2)

3.1. Methyl t-butyl ether (MTBE)

Photoionization and threshold measurements have been previously reported for MTBE [10]. We have carefully looked at PIE *versus* wavelength for room temperature samples of MTBE and of its deuterated analogue $(CH_3)_3COCD_3$ (MTBE-d_3) and find 298 K AEs of 9.31 ± 0.02 and 9.33 ± 0.02 eV, respectively, for the M–CH_3· fragment ions (*m/z* 73 and *m/z* 76). These AEs do not differ significantly from one another and are identical to the respective adiabatic ionization energies for the much less intense parent

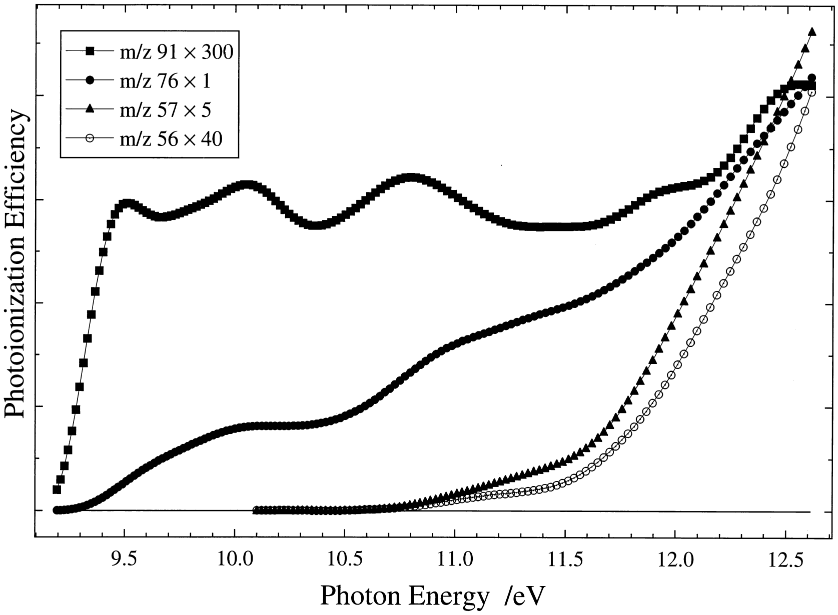

Fig. 2. Photoionization efficiency (PIE) as a function of wavelength for room temperature $(CH_3)_3COCD_3$ (MTBE-d_3) as a function of ionizing energy. The PIE curve was fitted using 15-point FFT smoothing.

ions ($M^{+\cdot}$ = *m/z* 88 for MTBE and *m/z* 91 for MTBE-d_3). PIE curves for MTBE-d_3 are shown in Fig. 2. In the jet-cooled apparatus ($\lambda = 118$ nm; $h\nu = 10.45$ eV) the $M^{+\cdot}$ intensity is much higher (roughly one-tenth the M–CH_3· ion abundance) than at any wavelength in the PIE curve using room temperature samples. Heating MTBE prior to jet expansion, however, increases its energy content sufficiently that $M^{+\cdot}$ can no longer be detected. Increasing the MTBE concentration in the room temperature molecular beam (which reduces the cooling efficiency of supersonic expansion) also diminishes the intensity of $M^{+\cdot}$ from MTBE.

Thermodynamically, molecular elimination of methanol to yield isobutene is much less endothermic than C–C bond homolysis. The DFT electronic energy of the homolysis products is 2.83 eV above that of the molecular elimination products (Table 1). Even taking into account the fact that the experimental activation barrier for molecular elimination is 1.9 eV greater than the thermodynamic threshold [2], molecular elimination should operate to the virtual exclusion of homolysis for homogeneous gas phase decomposition at temperatures below 1000 °C.

Pyrolysis/jet expansion/photoionization-TOF mass spectra of MTBE-d_3 are summarized by the stack plot in Fig. 3. Below a nominal temperature of 900 °C the observed spectra are consistent with molecular elimination of methanol-d_3 to form isobutene. However, at a nominal temperature of 900 °C peaks from ionization of methyl radical (*m/z* 15) and CD_3 radical (*m/z* 18) begin to appear with equal intensity. Methyl radicals do form at this nozzle temperature as a result of thermal decomposition of isobutene, but in a separate pyrolysis experiment with isobutene they are observed to have a lower abundance relative to the isobutene molecular ion (*m/z* 56) than we see in the MTBE and MTBE-d_3 pyrolyses. Therefore we infer that MTBE must be cleaving directly to form methyl radicals. Pyrolysis of MTBE-d_3 at a nominal temperature of 1000 °C gives more prominent CH_3 and CD_3 peaks. The *m/z* 15 ion intensity from isobutene pyrolysis at a nominal temperature of 1000 °C is roughly 10% that of *m/z* 56, while the 1000 °C trace in Fig. 3

exhibits an m/z 15 peak whose intensity is closer to 25% that of m/z 56. Moreover, the presence of m/z 18 (which does not form from pyrolysis of methanol-d_3) confirms that MTBE-d_3 must be undergoing bond homolysis at nominal temperatures ≥900 °C.

3.2. t-Octyl methyl ether (TOME)

The sample of TOME used for this study contained a small amount of alkenes from the starting material (2,4,4-trimethylpentenes, $mw = 112$), but that impurity did not interfere significantly with these experiments for two reasons: (1) the GC/MS of TOME exhibits a negligible m/z 112 fragment, so that the presence of this ion in TOME's photoionization mass spectrum can be wholly ascribed to the presence of these alkenes; and (2) the alkenes display less thermal stability than TOME. At a nominal temperature of 700 °C >95% of the m/z 112 from the trimethylpentene impurity has gone away, while less than half of the TOME has decomposed. In fact, the presence of 2,4,4-trimethyl-1-pentene in the TOME sample permits a qualitative assessment of the fate of TOME's molecular elimination products.

Table 1
DFT electronic energies (B3LYP/6-31G**//B3LYP/6-31G**) for relevant molecules, free radicals, and cations. Except where specified, no symmetry constraints were imposed on the geometry optimization. Energies in atomic units (1 a.u. = 27.21 eV).

	mw	E^{el} (a.u.)
$CH_3\cdot$ (D_{3h})	15	-39.842880
CH_3OH (C_s)	32	-115.723965
$(CH_3)_2C{=}CH_2$ (C_s)	56	-157.238836
$(CH_3)_3CCH_2\cdot$	71	-197.114968
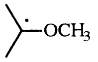	73	-233.016005
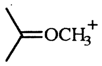	73	-232.809815
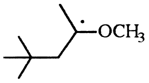	129	-390.280918
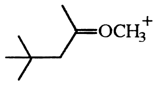	129	-390.081629

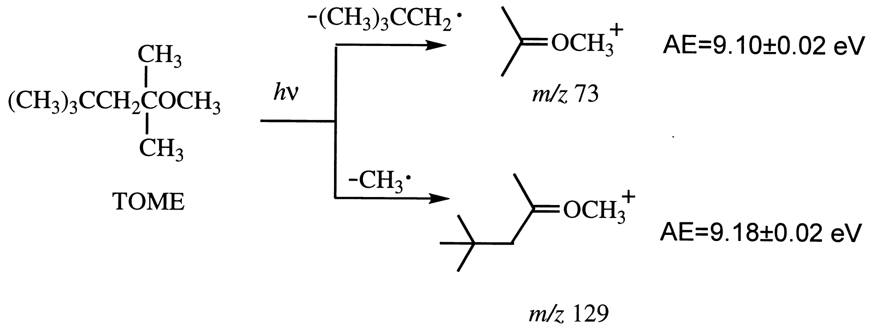

(3)

Consider the homolysis of C–C bonds. This process dominates the dissociation of ionized TOME (whose molecular ion, m/z 144, was not observed under any of the photoionization conditions examined here). Eq. (3) summarizes the two competing homolyses of the radical cation. The lower energy process expels a neopentyl radical, $(CH_3)_3CCH_2\cdot$, to form an O-methylated acetone ion, $(CH_3)_2C{=}OCH_3^+$ (m/z 73). The higher energy process expels a methyl radical to form O-methylated neopentyl methyl ketone. The experimental appearance energies differ by 0.08 eV. That difference agrees qualitatively with DFT calculations (B3LYP/6-31G**; electronic energies summarized in Table 1), which predict that m/z 73 plus

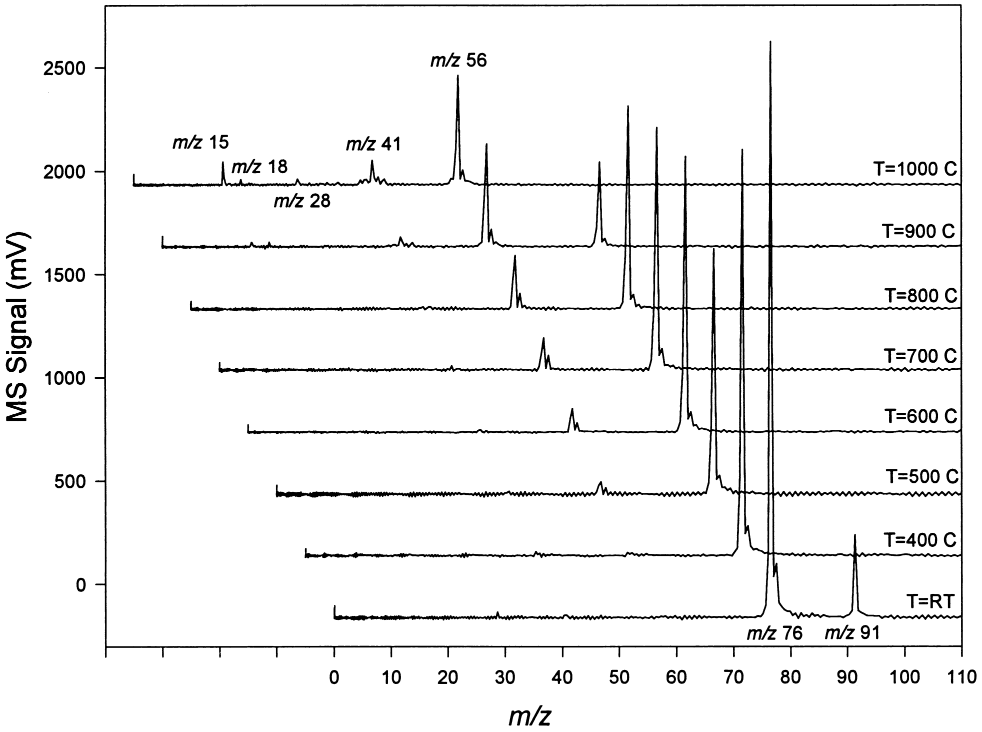

Fig. 3. Stack plot of pyrolysis/supersonic jet expansion/118 nm photoionization TOF mass spectra of MTBE-d_3 as a function of nominal temperature. Nozzle temperature is related to the nominal temperature by the empirical expression given in Sec. 2. Peaks from the expansion gas (argon) have been subtracted.

neopentyl radical have an electronic energy 0.008 eV lower than *m/z* 129 plus methyl radical. The relative abundance of these two ions varies as a function of ionizing energy, as a plot of their intensity ratio shows in Fig. 4.

Now suppose the neutral molecule were to undergo homolysis to give a pair of free radicals. Four possible simple C–C bond fissions might occur, as the squiggly lines in Eq. (4) portray. Either of two methyl cleavages (labeled *i* and *iv*) would produce neutral methoxydimethylpentyl radicals (MW 129). Alternatively, a *t*-butyl radical (MW 57) might break off (*ii*) to form a methoxyisobutyl radical (MW 87). Finally, a neopentyl radical (MW 71) might split apart (*iii*) from a methoxyisopropyl radical (MW 73). Fission *iii* gives the most stable products: DFT calculations place their electronic energy 0.20 eV lower than the products of fission *iv*. We detect no ions corresponding to the free radical masses except for *m/z* 73 and 129 (which also come from photoionization of TOME) and *m/z* 15 and 57, which also come from thermal decomposition of 2,2,4-trimethylpentenes (the alkenes produced by molecular elimination of

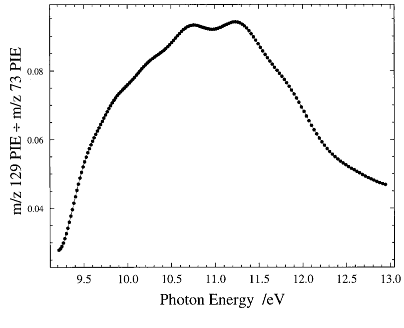

Fig. 4. Fragment ion intensity ratio of M–CH_3 (*m/z* 129) to M–C_5H_{11} (*m/z* 73) ions from photoionization of room temperature $(CH_3)_3CCH_2C(CH_3)_2OCH_3$ (TOME) as a function of ionizing energy. The PIE ratio curve was fitted using 20-point FFT smoothing.

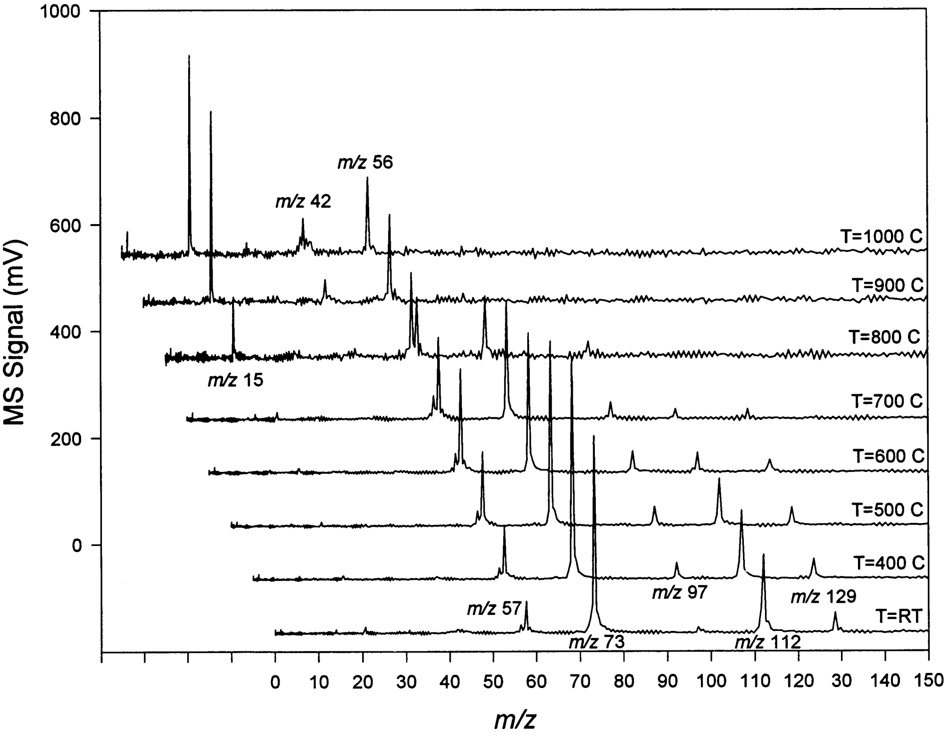

Fig. 5. Stack plot of pyrolysis/supersonic jet expansion/118 nm photoionization TOF mass spectra of TOME as a function of nominal temperature. Nozzle temperature is related to the nominal temperature by the empirical expression given in Sec. 2. Peaks from the expansion gas (argon) have been subtracted.

methanol from TOME). The TOME data do not support the inference of any of the homolyses depicted in Eq. (4)

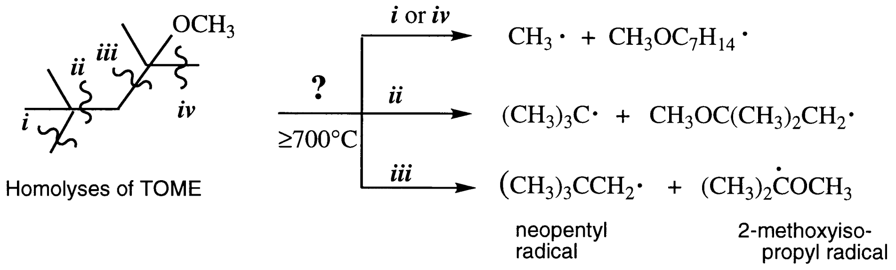

(4)

Pyrolysis of TOME as a function of nominal temperature is shown by the stack plot of supersonic jet/photoionization TOF mass spectra in Fig. 5. Interpreting the gradual diminution of the most intense peak (*m/z* 73) poses the first question. If homolysis *iii* were operating, it would serve to increase the intensity of *m/z* 73 relative to other ions that come from the photoionization of intact TOME. However, up to 700 °C the *m/z* 129:*m/z* 73 intensity ratio remains constant, within experimental uncertainty, as the graph in Fig. 6 summarizes. This ion ratio also provides a crude thermometer, since it is quite sensitive (as Fig. 4 summarizes) to internal energy. The

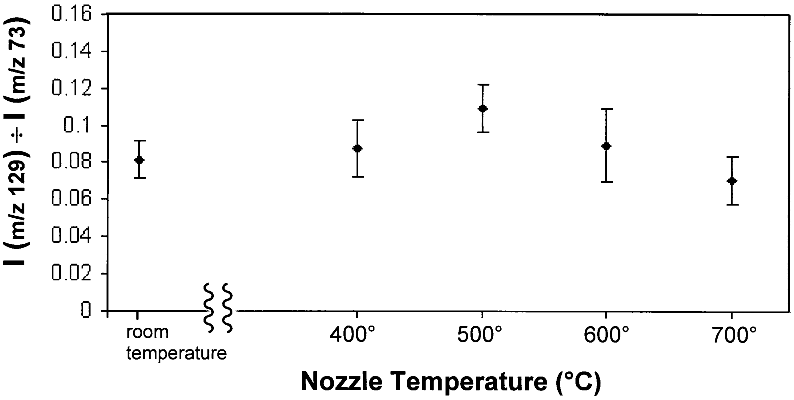

Fig. 6. [M–CH_3]:[M–C_5H_{11}] ion intensity ratio for pyrolysis/supersonic jet/118 nm photoionization TOF mass spectra of TOME as a function of nominal temperature, showing no significant variation. Nozzle temperature is related to the nominal temperature by the empirical expression given in Sec. 2. Error bars stand for sample standard deviations.

thermal vibrational energy content of neutral TOME at room temperature is calculated to be between 0.25 and 0.3 eV. At 700 °C the thermal vibrational energy content of neutral TOME is approximately 2.5 eV. Supersonic jet cooling appears to be efficient enough to remove ≥80% of that internal energy; otherwise the *m/z* 129: *m/z* 73 intensity ratio would have been expected to show a significant increase. We reject the implausible notion that heating of neutral TOME along with homolyses *i*, *iii*, and *iv* fortuitously operate together so as to leave that ion ratio unchanged.

At nominal temperatures between 400 °C and 600 °C the variation of hydrocarbon ions from TOME pyrolysis gives no evidence of their being produced from TOME. The *m/z* 112 intensity falls off by a factor of roughly 5, as would be predicted for pyrolysis of the 2,4,4-trimethylpentene impurities alone. At the same time splitting of a methyl radical off of neutral 2,4,4-trimethyl-2-pentene leads to an *m/z* 97 ion, whose intensity slowly builds up, just as one would expect for decomposition of the equilibrium alkene mixture. In this same temperature interval *m/z* 57 (which comes from the major thermal decomposition pathway of 2,4,4-trimethyl-1-pentene) appears, if anything, *less* intense than would have been expected from pyrolysis of the alkene impurities.

We compare the thermal decomposition of TOME with that of 2,4,4-trimethyl-1-pentene and of 2,4,4,-trimethyl-2-pentene (whose spectra are not shown here). In going from room temperature to a nominal temperature of 600 °C less than 40% of the TOME decomposes (judging from the *m/z* 73 intensity, which has to correspond to an oxygen-containing ion). At higher temperatures, however, we see evidence for elimination of methanol. At 700 °C the intensity of *m/z* 112 is about three times higher than would be expected from 2,4,4-trimethylpentene impurities by themselves. This result accords with what we should anticipate for 2,4,4-trimethylpentene that comes from thermolysis of TOME: the product alkene has a shorter mean contact time than the alkenes initially present and therefore exhibits a lower extent of thermal decomposition. At still higher temperatures the ions that become prominent—*m/z* 15, 41, and 56—are the same ones (and in the correct proportions) as in pyrolysis of the alkenes. There is no evidence in these experiments for any direct products of TOME's thermal decomposition apart from the alkenes that arise via molecular elimination.

4. Discussion

t-Alkyl methyl ethers exhibit a high degree of thermal stability under homogeneous gas phase conditions. From its reported Arrhenius parameters ($E_a = 2.56 \pm 0.04$ eV; $A = 10^{13.9}$ s^{-1}) [2], MTBE should have a half-life $<10^{-5}$ s at 1200 °C (the approximate nozzle temperature corresponding to a nominal temperature of 1000 °C). Experimentally we find that MTBE completely decomposes in a heated silicon carbide tube at that temperature. Bond homolysis is observed in competition with molecular elimination from MTBE at nominal temperatures ≥900 °C. On the one hand, if bond homolysis displayed the same preexponential factor as molecular elimination, expulsion of methanol from neutral MTBE would be expected to occur about 1500 times faster at 1200 °C than C–C bond fission. On the other hand, eight independent studies of the thermal decomposition of neopentane [2,3] (the closest published analogue to C–C bond cleavage in MTBE) have reported preexponential factors $A > 10^{16}$. A greater value of the A factor for homolysis (between 10^2 and 10^3 times greater than the A factor for molecular elimination) compensates for the higher energy barrier and implies that C–C bond fission [the first step of Eq. (5)] should occur to a measurable extent at the highest temperatures examined in our experiments.

We observe evidence for production of methyl radicals and CD_3 radicals in a ratio of roughly 1:1 at a nominal temperature of 900 °C (a nozzle temperature of approximately 1050 °C) and 3:1 at a nominal temperature of 1000 °C (a nozzle temperature of approximately 1200 °C), when correction is made for the *m/z* 15 contribution from thermal decomposition of isobutene. This can be ascribed to the sequence portrayed in Eq. (5): C–C bond fission of MTBE; then free radical dissociation of the resulting 2-methoxyisopropyl radical to acetone via loss of O-methyl; followed (at higher temperatures) by C–C bond homolysis of acetone with rapid, subsequent free radical dissociation to yield a pair methyl radicals. Separate experiments on acetone confirm that it decomposes extensively to methyl radicals (with carbon monoxide as the side product) in the silicon carbide nozzle at a nominal temperature of 1000 °C. The small peak at *m/z* 28 in the 1000 °C spectrum is assigned to CO that has been ionized by photoelectrons in the source (this peak is also observed in the pyrolysis/jet expansion/photoionization-TOF mass spectra of acetone and acetone-d_6).

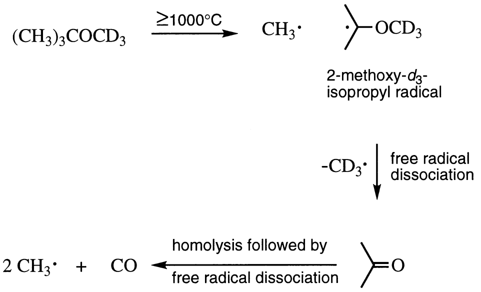

(5)

We conclude that MTBE produces free radicals directly via C–C bond fission, as drawn in the first step of Eq. (5). However, we do not observe production of free radicals directly from TOME, since the alkenes from its molecular elimination readily undergo homolysis (as demonstrated by the emergence of *m/z* 57 and 97 at a nominal temperature of 400 °C via pyrolysis of the 2,4,4-trimethylpentene impurities), obscuring evidence for C–C bond cleavage of the parent ether. The alkenes that arise from expulsion of methanol from TOME have shorter contact times than the 2,4,4-trimethylpentene impurities that are initially present, so it is not possible to gauge the alkene isomer ratio from molecular elimination simply on the basis of the mass spectra of authentic samples (even though 2,4,4-trimethyl-1-pentene exhibits a cracking pattern that differs significantly from that of 2,4,4-trimethyl-2-pentene).

Methoxyisopropyl cations constitute ≥90% of the total ionization from MTBE, MTBE-d_3, and TOME when the neutral ethers are photoionized at wavelengths longer than 105 nm. To judge from ion intensities as a function of temperature, TOME exhibits less thermal stability than MTBE. At a nominal temperature of 800 °C the *m/z* 73 peak from TOME is approximately 30% as intense as it is at room temperature, while the *m/z* 76 peak from MTBE-d_3 is closer to 40% of its room temperature intensity. At a nominal temperature of 900 °C no oxygen-containing peaks remain visible from TOME, while the *m/z* 76 peak from MTBE-d_3 retains 15% of its room temperature intensity.

DFT calculations predict that bond fission *iii* to form 2-methoxyisopropyl radical from neutral TOME is 0.2 eV less endothermic than cleavage of a methyl radical. Therefore C–C homolysis might onset at a lower temperature for TOME than is observed for MTBE. Evidence presented here argues against direct homolysis of TOME at nominal temperatures ≤700 °C, since the *m/z* 73: *m/z* 129 ion intensity ratio remains the same as for TOME itself. At nominal temperatures ≥800 °C, however, *m/z* 129 is no longer visible above noise level, so it is conceivable that some portion of *m/z* 73 at 800 °C arises via direct formation of methoxyisopropyl radicals followed by their photoionization. Assessing TOME's propensity for direct homolysis in further detail will require synthesis of isotopically labeled analogues.

Acknowledgements

The authors are grateful to Joseph A. Baker for synthesizing TOME and to Matt McCormick for help in designing and fabricating the pyrolysis source, as well as to the late Professor Bryan Kohler, whose laboratory provided much of the apparatus used for these experiments. This work was supported by NSF Grant Nos. CHE 99-83610 and 98-11400, by the Australian Research Council, by grants from the University of California Energy Institute, and by a block grant of Cray T90 computing time from the San Diego Supercomputing Center/NPACI.

References

[1] M.J. Papachristos, J. Swithenbank, G.H. Priestman, S. Stournas, P. Polysis, E. Lois, J. Inst. Energy 64 (1991) 113.
[2] J.E. Taylor, D.A. Hutchings, K.J. Frech, J. Am. Chem. Soc. 91 (1969) 2215.
[3] A.C. Baldwin, K.E. Lewis, D.M. Golden, Int. J. Chem. Kinet. 11 (1979) 529.
[4] V. Subba Rao, G.B. Skinner, Int. J. Chem. Kinet. 20 (1979) 165.
[5] K.Y. Choo, D.M. Golden, S.W. Benson, Int. J. Chem. Kinet. 6 (1974) 631.
[6] D.W. Kohn, H. Clauberg, P. Chen, Rev. Sci. Instrum. 63 (1992) 4003.
[7] H. Clauberg, D.W. Minsek, P. Chen, J. Am. Chem. Soc. 114 (1992) 99.
[8] S.W. Wright, D.L. Hageman, A.S. Wright, L.D. McClure, Tetrahedron Lett. 38 (1997) 7345.
[9] E.D. Hughes, C.K. Ingold, V.J. Shiner, J. Chem. Soc. (1953) 3827.
[10] J.C. Traeger, Rapid Commun. Mass Spectrom. 10 (1996) 119.
[11] J.C. Traeger, T.H. Morton, J. Am. Chem. Soc. 118 (1996) 9661.
[12] J.C. Traeger, A. Luna, J.C. Tortajada, T.H. Morton, J. Phys. Chem. A 103 (1999) 2348.
[13] W. Beveridge, J.A. Hunter, C.A.F. Johnson, J.E. Parker, Org. Mass Spectrom. 27 (1992) 543 and references therein.